
Figures and figure supplements

Structure and mechanistic features of the prokaryotic minimal RNase P

Rebecca Feyh et al

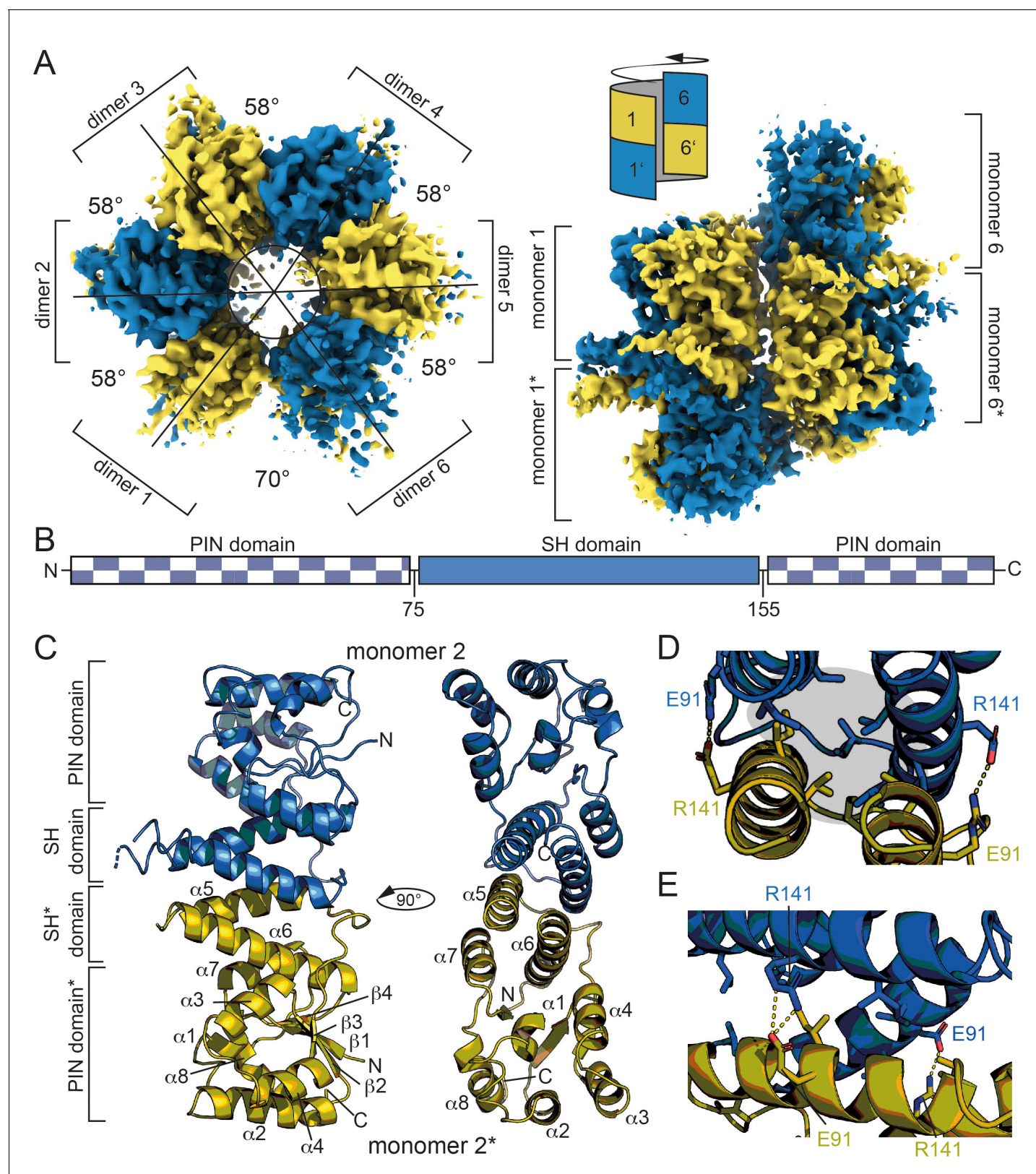


Figure 1. Dodecameric structure of Hhal2243. (A) Cryo-EM electron density map of Hhal2243 shown from a top view (left) and a side view (right). The monomers are colored in blue and olive, respectively. The angles between dimers are indicated in the top view. The sketch in the upper left corner of the view on the right indicates how the dimers assemble to form the screw-like arrangement of the dodecamer. (B) Domain architecture of Hhal2243. Figure 1 continued on next page

Figure 1 continued

(C) Model of the Hha12243 dimer. The protein consists of a PIN five domain with an inserted spike-helix (SH) domain forming the dimer interface. The numbers indicate the amino acid boundaries of the SH domain. (D, E) Detailed view of the dimer interface. The clamping salt bridges are shown as sticks and indicated with dashed yellow lines. The hydrophobic core between the two monomers is marked by the gray sphere in (D). EM, electron microscopy.

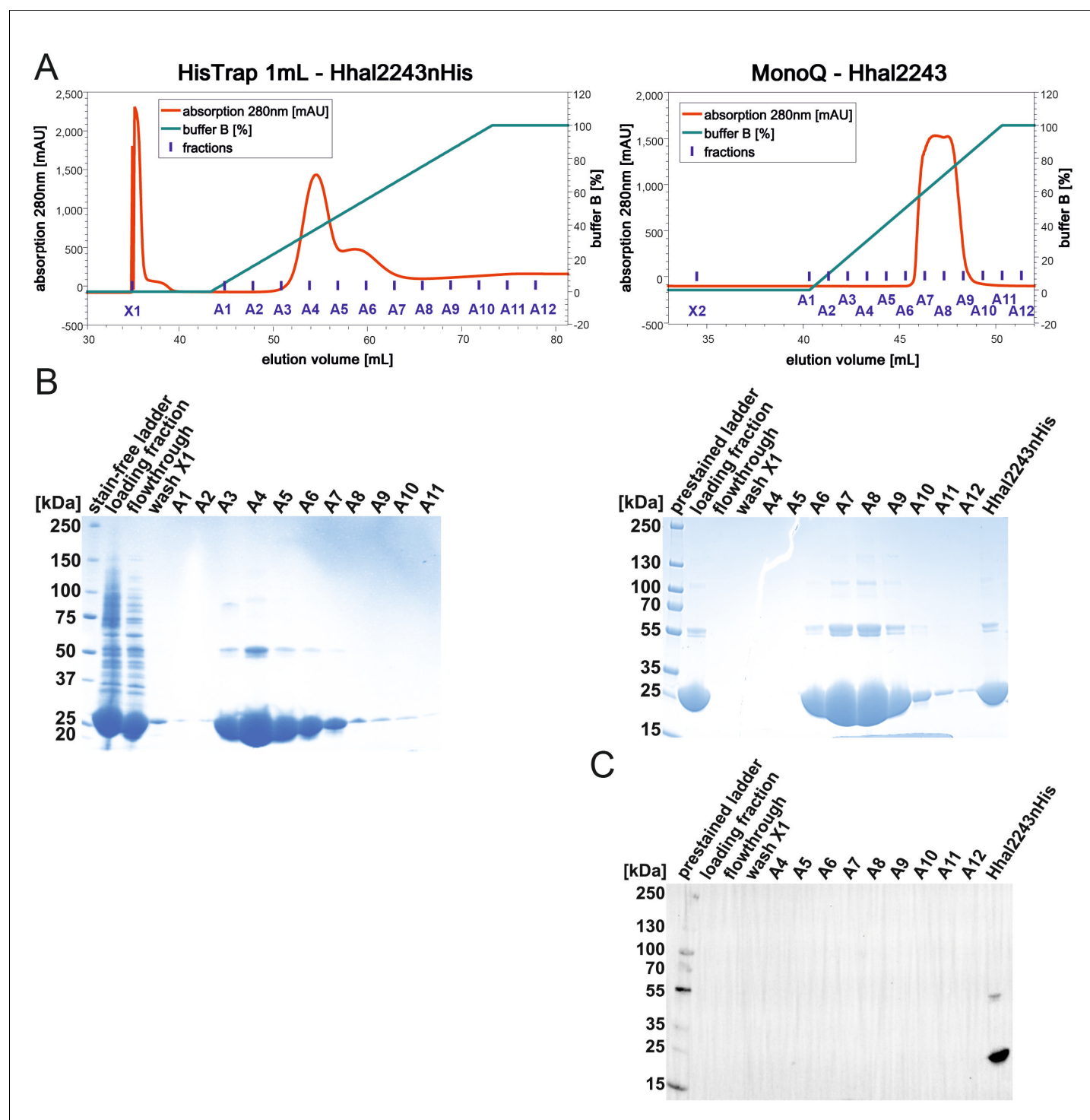


Figure 1—figure supplement 1. Purification of HhaI2243. (A) Chromatograms of the Ni-ion-affinity chromatography (HisTrap 1 mL column, left) and ion-exchange chromatography (MonoQ column, right). (B) SDS-PAGEs of fractions from the HisTrap (left) and MonoQ column (right). (C) Western blot analysis of fractions from the MonoQ column to verify successful removal of the His6-tag by thrombin digestion using an α -6His-HRP antibody (Thermo Fisher Scientific, Invitrogen) diluted 1:5000 in 1% Casein Blocker (Thermo Fisher Scientific). Source data of the SDS-PAGEs and the western blot are available in **Figure 1—figure supplement 1—source data 1**.

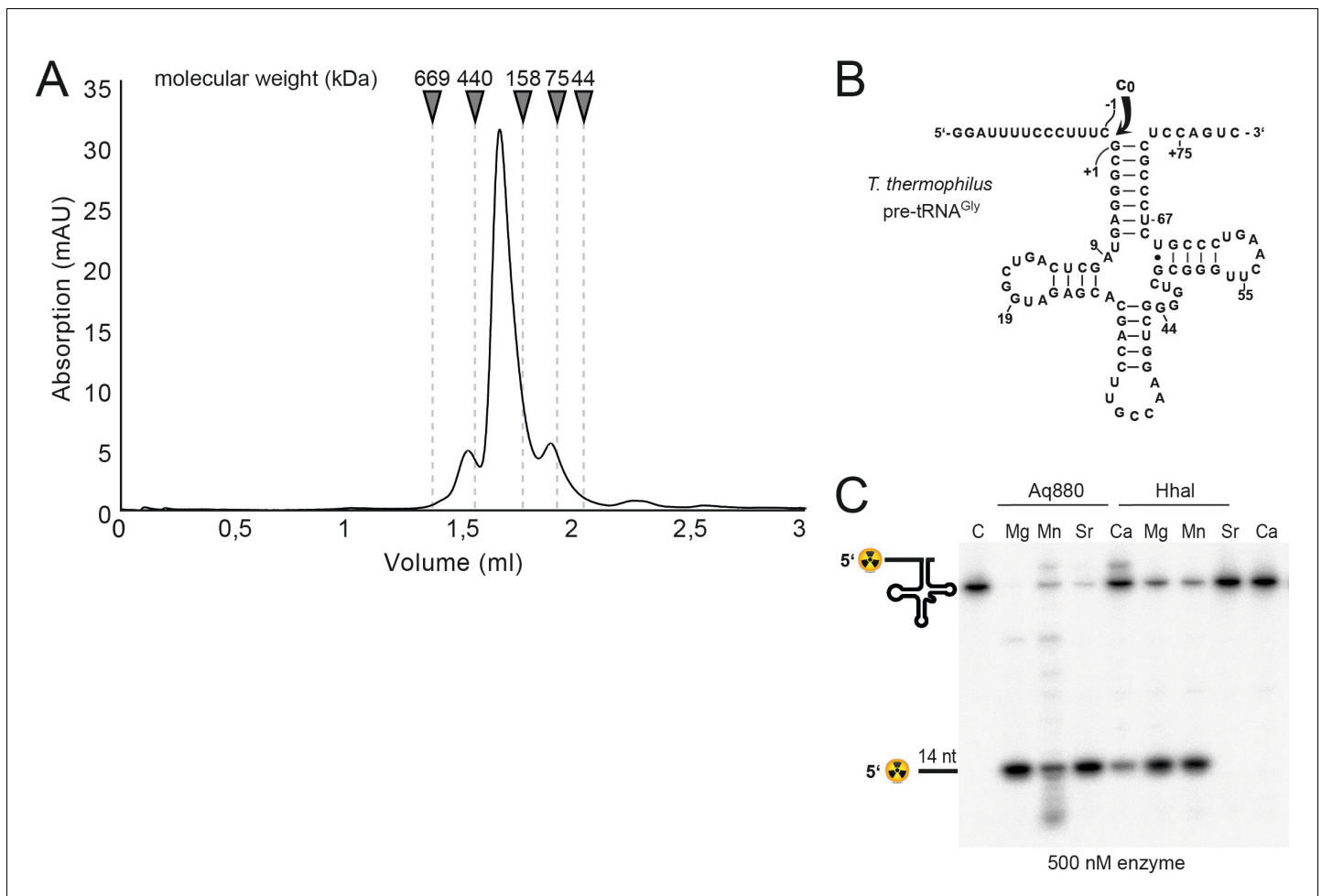


Figure 1—figure supplement 2. Analysis of Hhal2243. (A) Chromatographic analysis of Hhal2243. The sample was analyzed on a Superose 6 3.2/300 column using an ÄKTA PURE (GE Healthcare) FPLC system operated at room temperature. (B) Secondary structure of precursor tRNA^{Gly} (pre-tRNA^{Gly}) of the thermophilic bacterium *Thermus thermophilus* carrying a 5′-leader of 14 nucleotides; the curved arrow indicates the canonical (C₀) RNase P cleavage site. (C) RNase P processing of 5′-³²P-labeled *T. thermophilus* pre-tRNA^{Gly} by recombinant HARPs from the hyperthermophilic bacterium *A. aeolicus* (Aq880) and the γ -proteobacterium *Halorhodospira halophila* (Hhal2243) in the presence of either 4.5 mM Mg²⁺, Mn²⁺, Sr²⁺ or Ca²⁺ in buffer F for 2 hr at 37°C. Enzyme and substrate concentrations were 500 nM and ~5 nM, respectively. Samples were separated by 20% denaturing PAGE and analyzed by phosphor imaging (for details, see Materials and methods of the main text). C, control, substrate alone incubated for 2 hr at 37°C in enzyme dilution buffer (30 mM Tris-HCl pH 7.8, 30 mM NaCl, 0.3 mM EDTA, and 1 mM DTT). Source data of phosphor images are available in **Figure 1—figure supplement 2—source data 1**.

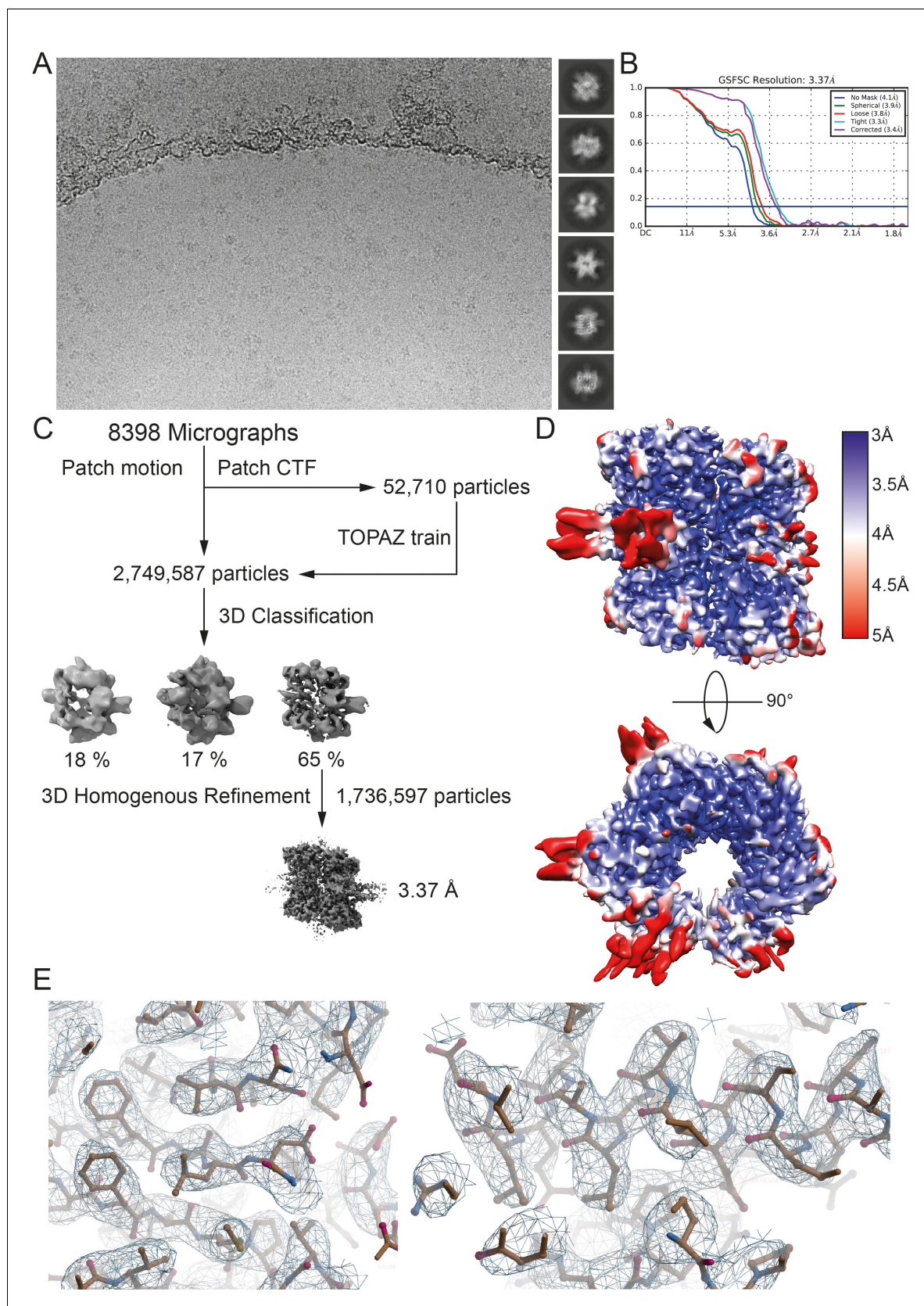


Figure 1—figure supplement 3. Cryo-EM data collection and analysis. (A) Representative cryo-EM micrograph collected with a Thermo Fisher Scientific Titan Krios microscope, operated at 300 kV, and equipped with a K3 direct electron detector. Representative reference-free 2D class averages

Figure 1—figure supplement 3 continued on next page

Figure 1—figure supplement 3 continued

are shown on the right side of the micrograph. (B) FSC analysis of the dataset with the blue line representing the estimated global FSC of 3.4 Å. (C) The 2,749,587 **particles** from the dataset were 3D classified into three classes using a reference ab initio model generated in Cryosparc v3.1. The class consisting of the best aligning particles was selected for 3D homogenous refinement in Cryosparc resulting in a final map at 3.37 Å resolution. (D) Local resolution estimation of the final map colored from blue (3 Å) to red (5 Å). (E) Representative images of the Hhal2243 model and surrounding electron density. Maps are displayed as mesh and contoured at 3σ . EM, electron microscopy.

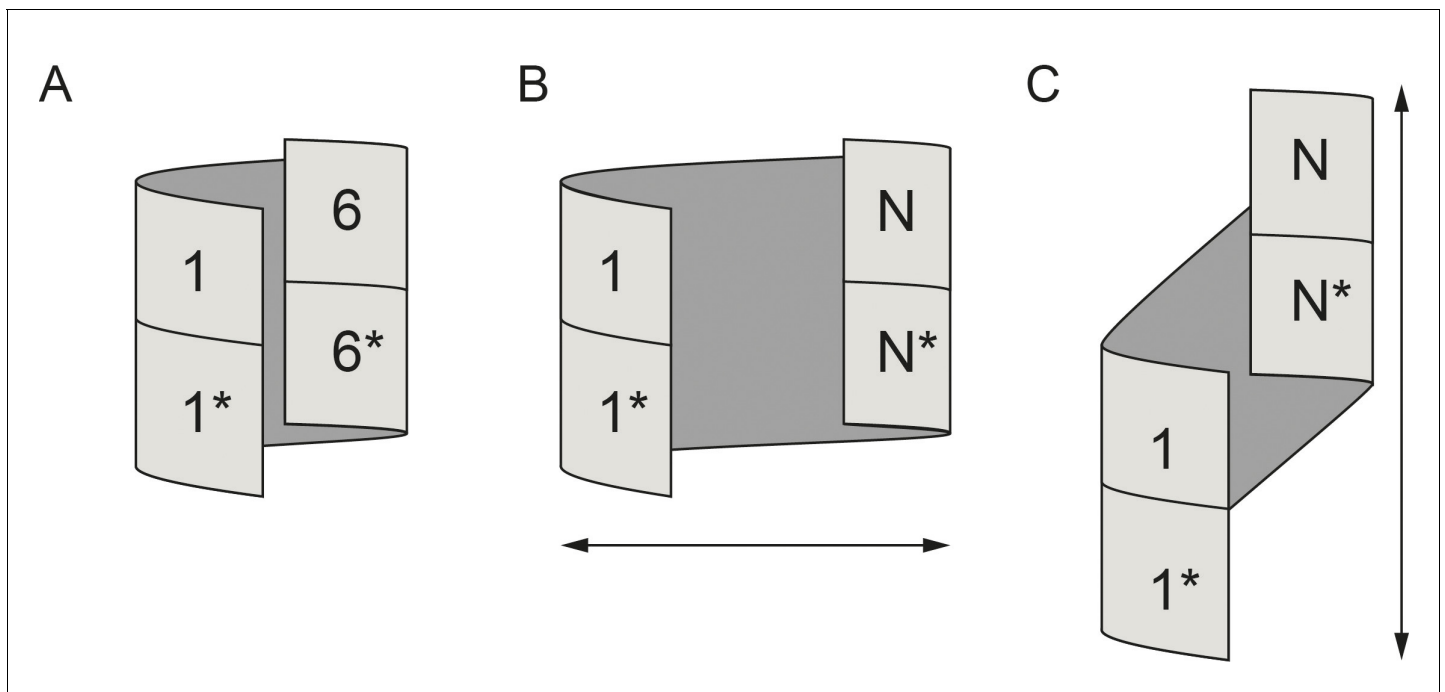


Figure 1—figure supplement 4. Hypothetical geometric scenarios of HARP oligomerization. (A) Geometry of the HARP dodecamer. (B, C) Hypothetic geometric scenarios that would allow a continuation of oligomerization beyond a dodecamer. In (B), the screw diameter would be expanded, while in (C) a helical pitch would be increased to such an extent that any steric interference between the first and last dimers is avoided.

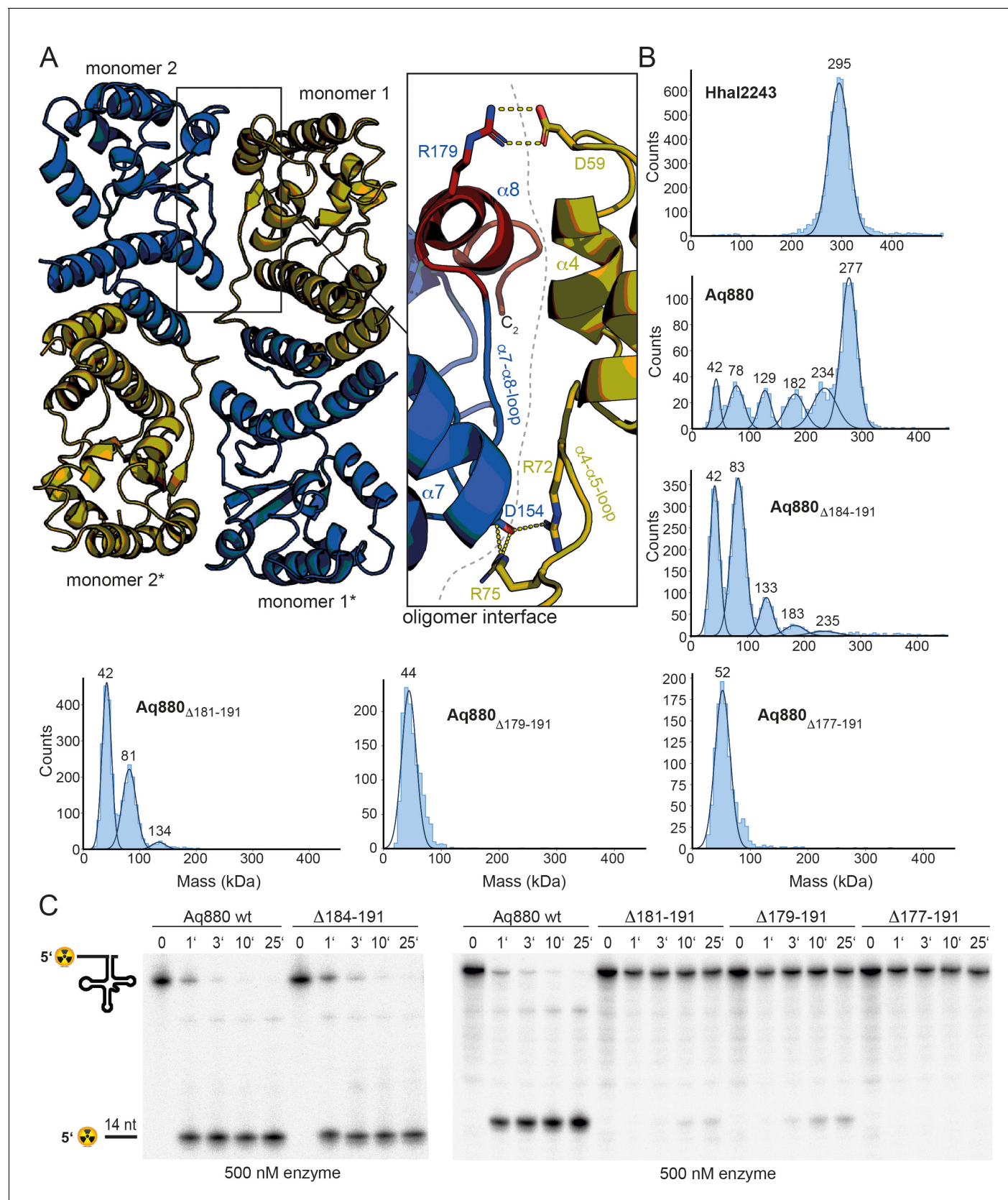


Figure 2. Oligomerization is required for HARP activity. (A) Oligomer interface between two monomers (colored in blue and olive) of interacting dimers. The C-terminus starting at residue 177 is colored in red to highlight the region deleted in the 'shortest' Aq880 variant ($\Delta 177-191$). Salt bridges

Figure 2 continued on next page

Figure 2 continued

are indicated with yellow dashed lines. **(B)** Mass photometry of Hhal2243, Aq880 wt, Aq880 $_{\Delta 184-191}$, Aq880 $_{\Delta 181-191}$, Aq880 $_{\Delta 179-191}$, and Aq880 $_{\Delta 177-191}$. Molecular masses corresponding to the respective Gaussian fits are shown in kDa above the fits. **(C)** Processing of pre-tRNA^{Gly} by Aq880 wt and derived mutant variants. Aliquots were withdrawn at different time points (1, 3, 10, or 25 min) of incubation at 37°C; 0, substrate without addition of enzyme. Aq880 wt in comparison with the C-terminal deletion variants $\Delta 177-191$, $\Delta 179-191$, $\Delta 181-191$, and $\Delta 184-191$, all at 500 nM enzyme. For more details, see Materials and methods. Source data of phosphor images are available in **Figure 2—source data 1**.

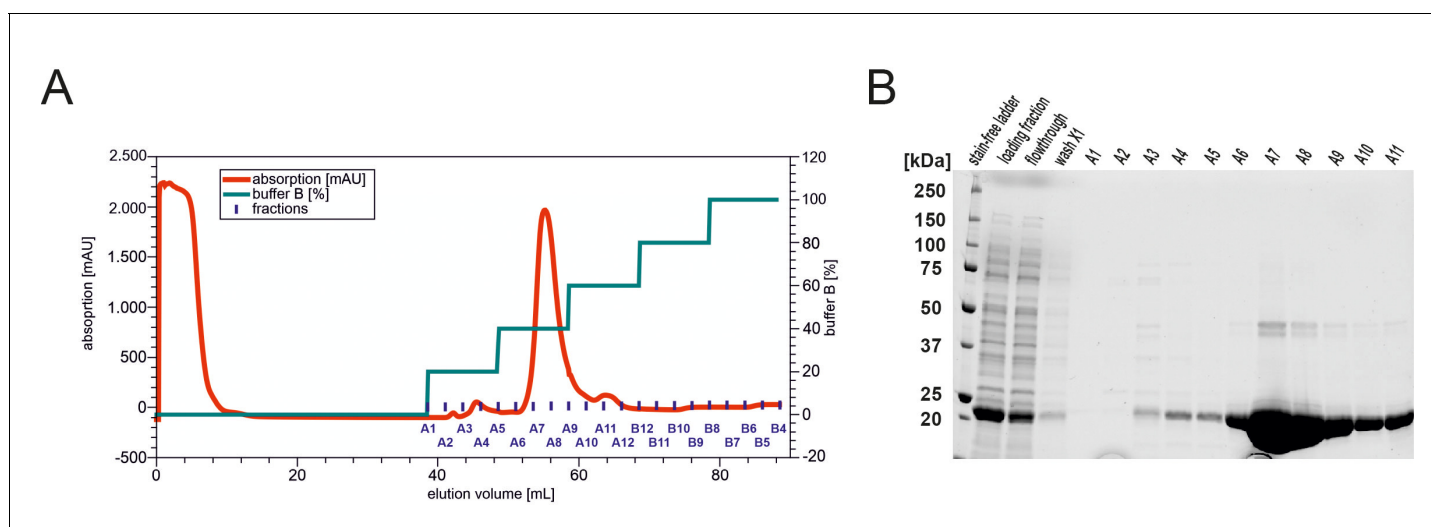


Figure 2—figure supplement 1. Purification of Aq880. (A) Chromatogram of the Ni-ion-affinity chromatography (HisTrap 5 mL column). (B) 12% TGX-gel of fractions from the HisTrap. Source data of the SDS-PAGEs are available in **Figure 2—figure supplement 1—source data 1**.

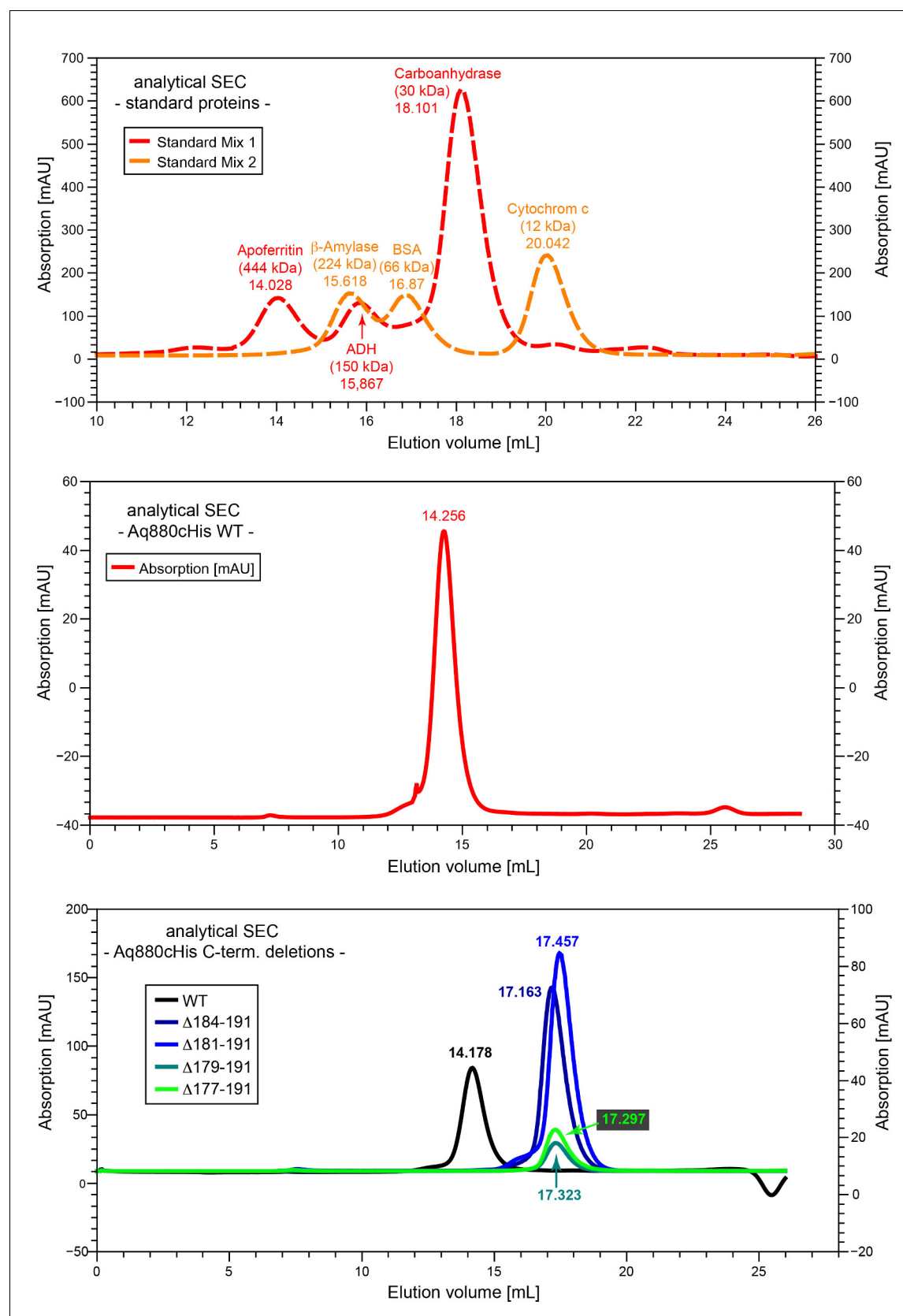


Figure 2—figure supplement 2. Chromatographic analysis of Aq880 WT and C-terminal deletion mutants. Samples were analyzed on a Superose 6 10/300 GL column using an ÄKTA Purifier (GE Healthcare) FPLC system operated at room temperature. The running buffer contained 20 mM Tris-HCl pH 7.5. Figure 2—figure supplement 2 continued on next page

Figure 2—figure supplement 2 continued

8.0, 100 mM KCl, 0.1 mM EDTA, and 3 mM DTT. The flow rate was 0.5 mL/min. (A) Overlay of two column runs with three marker proteins each, termed Standard Mix 1 and 2 (Gel Filtration Markers Kit for Protein Molecular Weights 12–200 kDa and Apoferritin, Merck Sigma-Aldrich). Identities of individual proteins and elution volumes of the respective peak fractions are indicated; ADH, alcohol dehydrogenase; BSA, bovine serum albumin. (B) Elution profile of Aq880 wt. (C) Elution profiles of C-terminal deletion variants of Aq880 lacking the indicated amino acids of the native protein. The elution profiles in panel A suggest an approximate mass of 430 kDa for Aq880 wt. The elution volumes of the C-terminal deletions mutants suggest molecular masses between ~55 and 68 kDa.

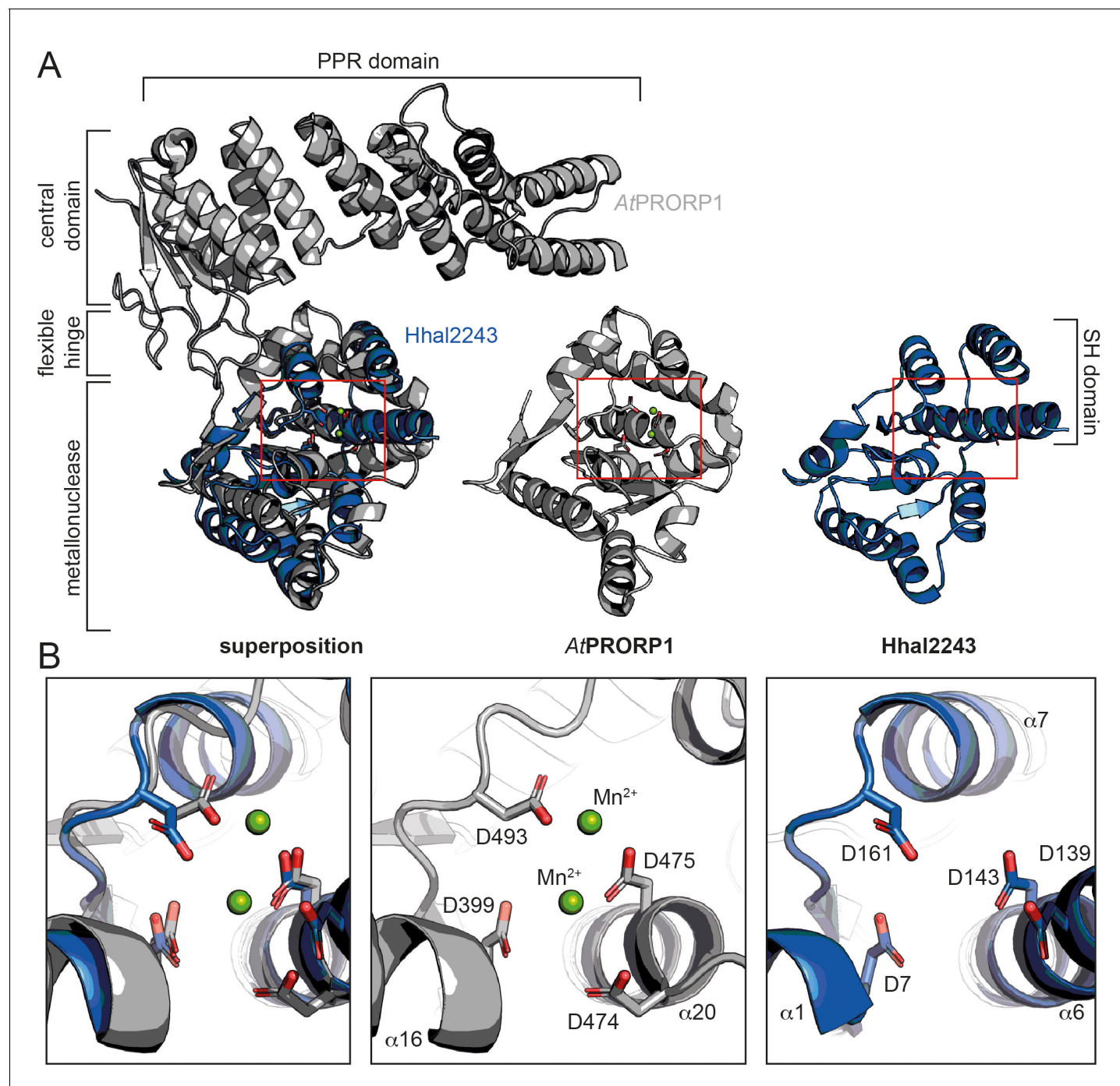


Figure 3. Comparison between HARP and PRORP systems. (A) Superposition of *AtPRORP1* (PDB: 4G24) and *Hhal2243* shows that the metallonuclease domain superposes well, while the PPR domain is absent in HARPs. The red rectangle shows the closeup in (B). (B) Orientation of active site residues is conserved among PRORPs and HARPs; the active site residues are positioned similarly in both enzyme types. *AtPRORP1* is colored in gray and *Hhal2243* in blue.

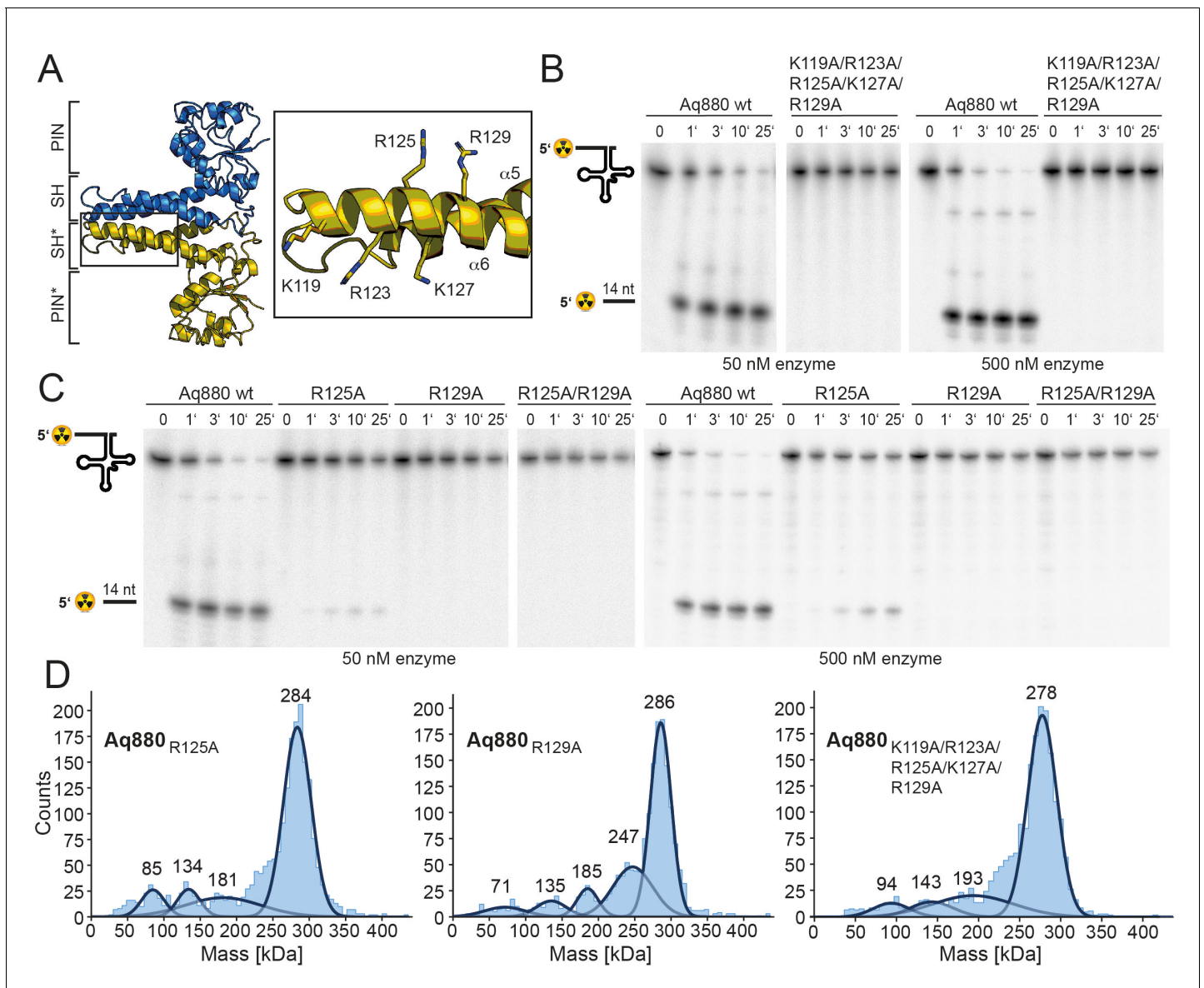


Figure 4. The SH domain is essential for RNase P activity. (A) Homology model of Aq880 with residues critical for pre-tRNA processing activity in the SH domain displayed as sticks. Processing of pre-tRNA^{Gly} by Aq880 wt and derived mutant variants. Aliquots were withdrawn at different time points (1, 3, 10, or 25 min) of incubation at 37°C; 0, substrate without addition of enzyme. (B) Aq880 wt and the quintuple mutant K119A/R123A/R125A/K127A/R129A at 50 nM (left) or 500 nM (right) enzyme; (C) Aq880 wt, the single mutants R125A and R129A, and the double mutant R125A/R129A, assayed at 50 nM (left) or 500 nM (right) enzyme. Source data of phosphor images are available in **Figure 4—source data 1**. (D) Mass photometry of Aq880_{R125A}, Aq880_{R129A}, and Aq880_{K119A/R123A/R125A/K127A/R129A}. Molecular masses corresponding to the respective Gaussian fits are shown in kDa above the fits. Source data of phosphor images are available in **Figure 4—source data 1**. SH, spike helix.

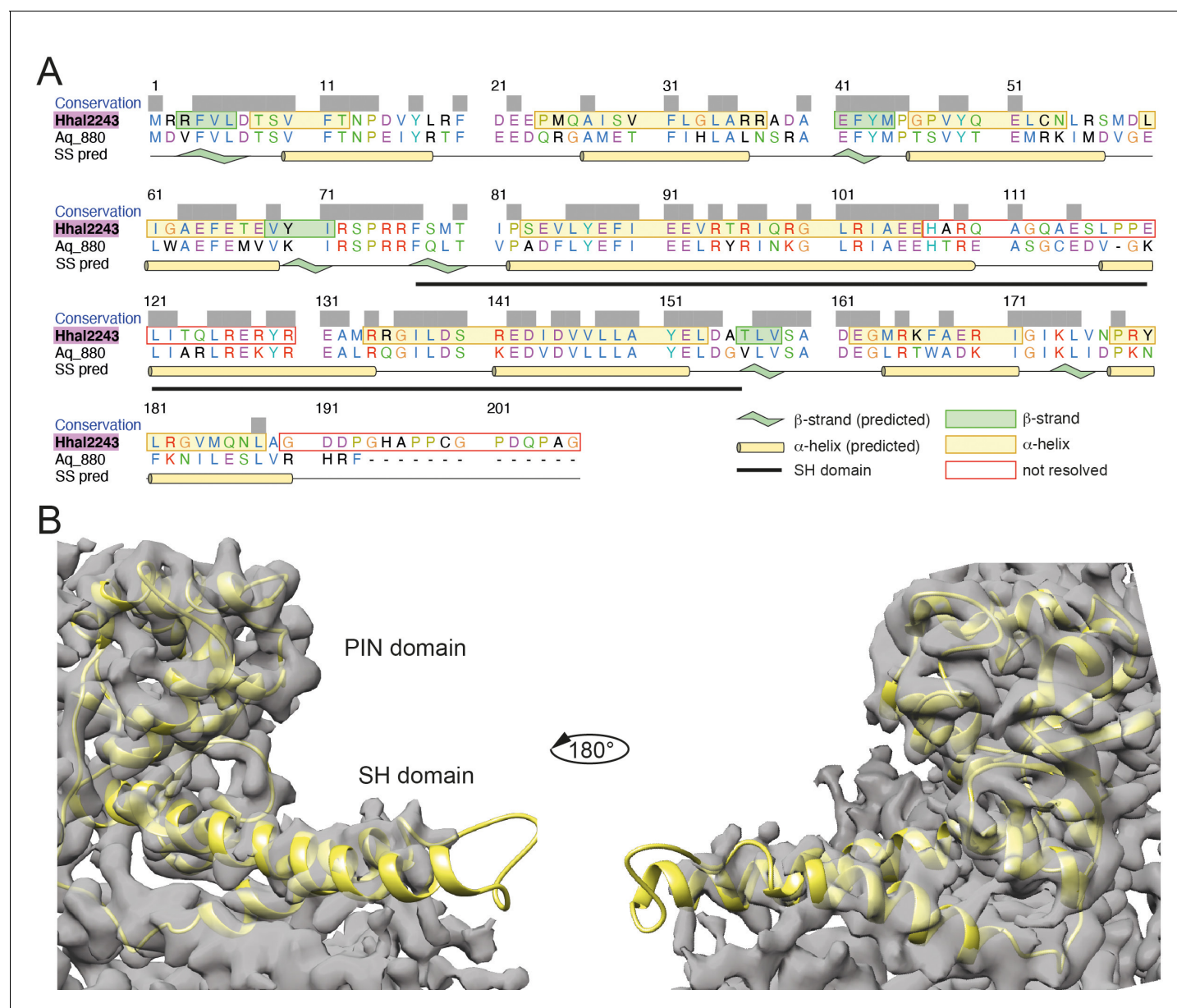


Figure 4—figure supplement 1. Homology model generation of Aq880. (A) Sequence alignment of Hhal2243 and Aq880. Secondary structure elements are drawn as observed in the cryo-EM structure of Hhal2243. The secondary structure prediction has been generated using PSIPRED (3) and is shown below the sequence alignment. The alignment colors are according to the physico-chemical properties of the respective amino acids. (B) Electron density map contoured at level 0.12 with the docked Aq880 model shown in yellow. EM, electron microscopy.

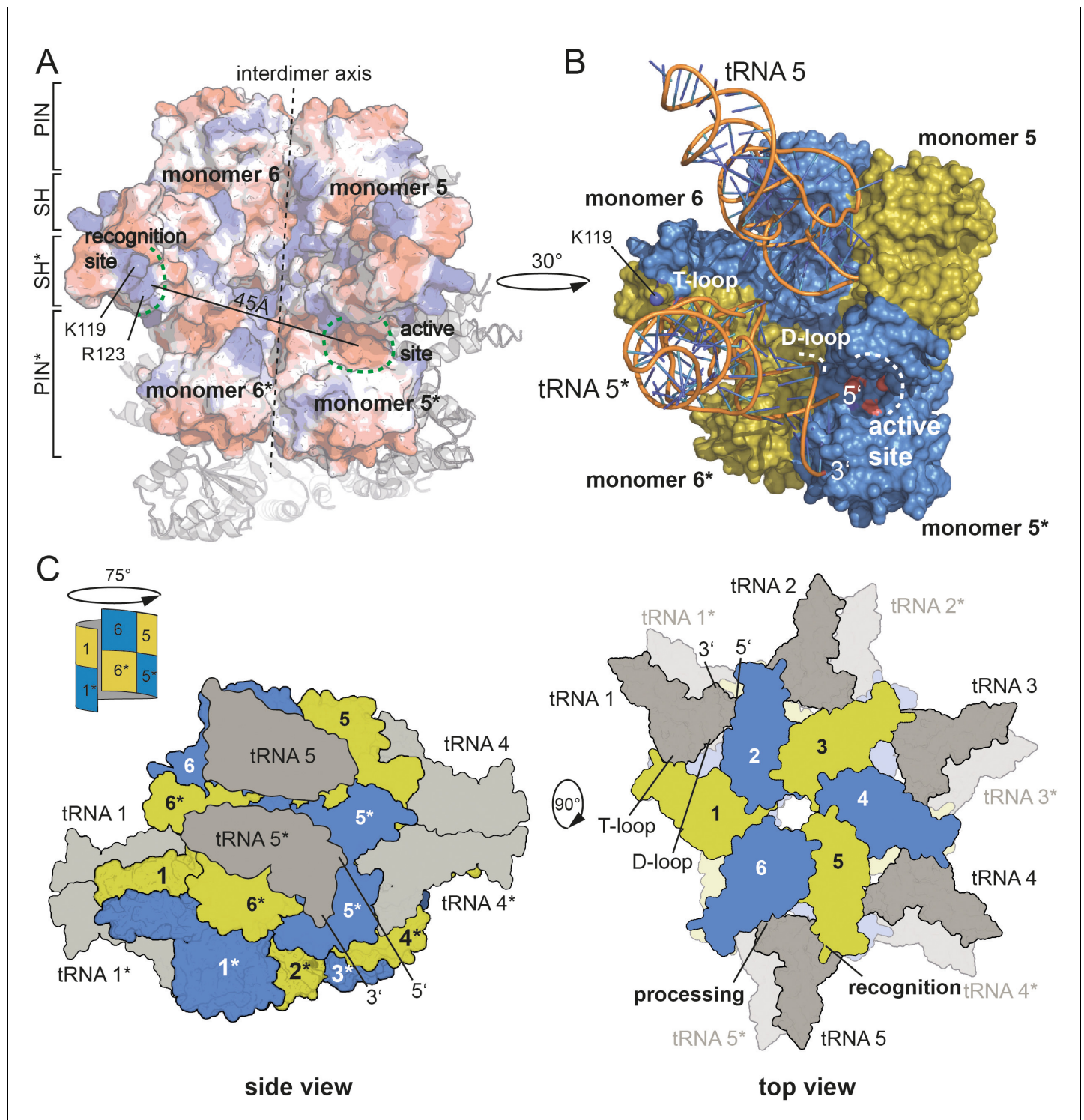


Figure 5. Model for tRNA recognition and processing by HARPs. (A) Surface of two adjacent Aq880 dimers colored according to the calculated electrostatic potential. The proposed recognition site for the tRNA elbow and the active site is indicated by curved dashed green lines; the distance between the two regions is approximately 45 Å. The almost vertical straight and dashed line marks the interdimer axis. The distance between the two regions is approximately 45 Å. The remaining subunits of the dodecamer are shown as cartoon in the background. (B) Closeup of the Aq880 surface colored in blue and olive. The tRNA^{Phe}, taken from the PRORP PPR domain co-structure (PDB: 6LVR), was docked onto our structure. The model predicts how the tRNA is coordinated by positive residues within the SH domain (of monomer 6* in this example) to position the 5'-end in close proximity to the active site of the neighboring dimer (of monomer 5* in this example). (C) Left: sketch of the Hha12243 homo-dodecamer with docked tRNAs. Right: top view of the dodecamer showing the arrangement of tRNAs and the processing and recognition sites.

Figure 5 continued

tRNAs as side view. The view is rotated by 75° compared to the view in **Figure 1A** indicated by a sketch in the upper left corner. Right: sketch of tRNA recognition and cleavage by HARPs shown from the top. Numbers indicate monomers.